HHS Public Access

Author manuscript

Andrology. Author manuscript; available in PMC 2018 November 01.

Published in final edited form as:

Andrology. 2017 November ; 5(6): 1141–1152. doi:10.1111/andr.12409.

Spontaneous testicular atrophy occurs despite normal spermatogonial proliferation in a *Tp53* knockout rat

Matthew S. Dai[1], **Susan J. Hall**[1], **Marguerite M. Vantangoli Policelli**[1], **Kim Boekelheide**[1], and **Daniel J. Spade**[1,2]

[1]Department of Pathology and Laboratory Medicine, Brown University, Providence, RI, USA

Abstract

The tumor suppressor protein p53 (TP53) has many functions in cell cycle regulation, apoptosis, and DNA damage repair, and is also involved in spermatogenesis in the mouse. To evaluate the role of p53 in spermatogenesis in the rat, we characterized testis biology in adult males of a novel p53 knockout rat (SD-*Tp53*^{tm1sage}). p53 knockout rats exhibited variable levels of testicular atrophy, including significantly decreased testis weights, atrophic seminiferous tubules, decreased seminiferous tubule diameter, and elevated spermatocyte TUNEL labeling rates, indicating a dysfunction in spermatogenesis. Phosphorylated histone H2AX protein levels and distribution were similar in the non-atrophic seminiferous tubules of both genotypes, showing evidence of pre-synaptic DNA double-strand breaks in leptotene and zygotene spermatocytes, preceding cell death in p53 knockout rat testes. Quantification of the spermatogonial stem cell (SSC) proliferation rate with bromodeoxyuridine (BrdU) labeling, in addition to staining with the undifferentiated type A spermatogonial marker GDNF family receptor alpha-1 (GFRA1), indicated that the undifferentiated spermatogonial population was normal in p53 knockout rats. Following exposure to 0.5 or 5 Gy X-ray, p53 knockout rats exhibited no germ cell apoptotic response beyond their un-irradiated phenotype, while germ cell death in wild-type rat testes was elevated to a level similar to the unexposed p53 knockout rats. This study indicates that seminiferous tubule atrophy occurs following spontaneous, elevated levels of spermatocyte death in the p53 knockout rat. This phenomenon is variable across individual rats. These results indicate a critical role for p53 in rat germ cell survival and spermatogenesis.

Keywords

p53; spermatogenesis; germ cell death

[2]Corresponding Author: Department of Pathology and Laboratory Medicine, Brown University, Box G-E5, 70 Ship St., Providence, RI 02912; tel: 401-863-2985; fax: 401-863-9008; daniel_spade@brown.edu.
DR. DANIEL J SPADE (Orcid ID : 0000-0002-4694-8724)

Disclosures

KB does occasional expert consulting with chemical and pharmaceutical companies. KB and SH own stock in a small start-up biotechnology company (Semma Therapeutics) developing a cell-based therapy for diabetes.

Author Contributions

DS, MD, & KB designed the experiments; MD, SH, MP, & DS performed the research; MD, MP, & DS analyzed data and wrote the paper; all authors edited and approved the paper.

Introduction

The tumor suppressor protein p53 (TP53, hereinafter referred to as p53) is encoded by the *Tp53* gene on rat chromosome 10 and by the homologous *TP53* gene on human chromosome 17. p53 has critical functions in the regulation of the cell cycle, including in apoptosis and cell cycle arrest, reviewed by Benchimol (2001) and Fridman & Lowe (2003). Following DNA damage, p53 causes cell cycle arrest and recruits proteins for DNA damage repair. After severe damage, p53 initiates apoptosis through activation of the caspase-9 pathway and transcriptional regulation of target genes. Apoptosis can be induced through DNA stress stimuli like oxidative stress, toxicant exposure, or ionizing radiation. p53 activity and regulation has been shown to be specific to cell type, developmental stage, and stimulus.

Through its functions in DNA damage repair, apoptosis, and cell cycle arrest, p53 mitigates DNA mutations and unregulated cell proliferation that can lead to cancer. In humans, germline *TP53* mutations lead to Li-Fraumeni syndrome, a rare but serious autosomal dominant disorder (Hollstein *et al.* 1991). Li-Fraumeni syndrome leads to significantly increased occurrence of brain cancers, breast carcinomas, sarcomas, leukemia, and adrenal tumors (Malkin *et al.* 1990; Malkin 1993). In p53 mutant mouse models, tumor frequency is increased in both haploid and complete p53 knockout mice (Venkatachalam *et al.* 2001). p53 knockout mice are susceptible to multiple tumor types. A germline mutant derived from mouse embryonic stem cell-C57BL/6 chimeras develops a tumor spectrum similar to Li-Fraumeni syndrome, consisting of predominantly sarcomas and lymphomas (Jacks *et al.* 1994). Recently, three p53 knockout rat models have been established using different background strains (Tong *et al.* 2010; van Boxtel *et al.* 2011), including a p53 knockout rat model (SD-*Tp53*^{tm1sage}) developed on a Sprague Dawley background through an 11-nucleotide deletion using pronuclear microinjection of zinc finger nucleases (ZFNs) (McCoy *et al.* 2013). Compared to knockouts established in other strain backgrounds, this Sprague Dawley model has demonstrated a broader tumor spectrum that more closely mirrors that of Li-Fraumeni syndrome.

p53 is involved in various other biological processes in addition to tumor suppression and apoptosis, including spermatogenesis. Spermatogenesis is characterized by high rates of germ cell mitosis, meiosis, and apoptosis, processes that involve roles for p53. p53 is induced during meiosis following the introduction of DNA double-strand breaks prior to homologous recombination (Lu *et al.* 2010). In p53 mutant mouse models, spermatogenesis is impaired at the level of spermatogonia or spermatocyte survival and proliferation (Rotter *et al.* 1993; Schwartz *et al.* 1993; Beumer *et al.* 1998; Golas *et al.* 2011). Germ cell apoptosis is an important phenomenon that occurs normally at a low rate in the testis, and is induced indirectly following exposure to Sertoli toxicants or directly by germ cell toxicants. Ionizing radiation, including both γ and X-radiation, directly leads to increased rates of germ cell apoptosis in mice and rats (Hasegawa *et al.* 1997; Richburg *et al.* 2000; Yamasaki *et al.* 2010), through a mechanism involving both p53 and Fas in the mouse. Notably, apoptotic response to X-radiation is reduced in p53-deficient mice (Hasegawa *et al.* 1997; Beumer *et al.* 1998; Embree-Ku *et al.* 2002). Further, apoptosis of spermatogonial stem cells (SSCs) is p53-dependent in the mouse (Coureuil *et al.* 2010; Ishii *et al.* 2014). In addition to the roles

of p53 in germ cells, p53 is expressed in Sertoli cells, has a role in establishing Sertoli cell maturation (Scherthan *et al.* 2000), and is responsible for Sertoli cell apoptosis in Sertoli cell-conditional Mdm2 knockout mice (Fouchecourt *et al.* 2016).

In the present study, we aimed to characterize the testicular biology, including spermatogenesis and seminiferous tubule development, as well as response to X-radiation, in the p53 knockout rat. Our goal was to improve the understanding of the roles of p53 in germ cell biology and spermatogenesis in the rat, which have not previously been characterized. While we hypothesized that p53−/− rats would be resistant to X-ray-induced germ cell apoptosis, we found that the non-irradiated p53−/− rat testis was characterized by variable levels of spontaneous spermatocyte death and seminiferous tubule atrophy.

Materials and Methods

Animals and Experimental Protocols

Male wild-type (p53+/+) and p53 knockout (p53−/−) rats (SD-*Tp53*^{tm1sage}, strain code TGRA3990) of Sprague-Dawley background (McCoy *et al.* 2013) were obtained from SAGE Laboratories (Boyertown, PA). Animals were housed in humidity- and temperature-controlled rooms and maintained on a 12:12 hour light-dark cycle, with food (Purina Rodent Diet 5010, PharmaServ, Inc., Framingham, MA) and water available *ad libitum*. All procedures involving animals were performed in accordance with the National Research Council's Guide for Care and Use of Laboratory Animals and were approved by Brown University's Institutional Animal Care and Use Committee (IACUC).

To characterize the testicular biology of p53 knockout rats, 60-day old male p53 knockout rats were continuously exposed to bromodeoxycytidine (BrdC) for 13 days via an Alzet Model 2001 micro-osmotic pump (Alzet Corp., Palo Alto, CA) implanted through a dorsal subcutaneous incision. Pumps were filled with 0.12 M BrdC in sterile-filtered phosphate buffered saline (PBS) and equilibrated overnight in sterile PBS at 37°C. Pumps were replaced after 6 days with identically filled pumps, and animals were euthanized on PND 73 by CO_2 asphyxiation after 13 days of continuous BrdC exposure. Wild-type rats were euthanized on PND 77 without BrdC exposure. For all rats, body, testis, and epididymis weights were recorded. A portion of the left testis was fixed in modified Davidson's fixative, transferred to 10% neutral buffered formalin after 24 h, and stored for later histological analysis, TUNEL assay, and immunohistochemistry (IHC) for γH2AX, BrdU, and cleaved caspase-3. A portion of the right testis was detunicated and fixed in 4% paraformaldehyde for GDNF family receptor alpha-1 (GFRA1) staining of whole mounted seminiferous tubules. In all analyses, the sample size was n=5 rats, with one testis per rat examined histologically.

To characterize the response of p53 knockout rats to X-radiation, 55–59-day old p53−/− and p53+/+ rats were exposed to a single dose of 0.5 or 5 Gy X-ray at a rate of 0.80–0.87 Gy/min using an RT 250 kVp X-ray machine (Philips, Best, Netherlands). Rats were placed in plastic restraints with a lead shield protecting the anterior half of the body. Control rats were held in exposure restraints for equivalent time with no X-ray exposure (0 Gy). At 3 h post-exposure, rats were anesthetized using flow-through isoflurane and hemi-castrated. The

left testis and epididymis were removed, and a portion of the excised testis was fixed in modified Davidson's fixative or 10% neutral buffered formalin. Samples fixed in modified Davidson's fixative were transferred to 10% neutral buffered formalin after 24 h. 12 h (5 Gy-exposed rats) or 6 weeks (42 or 43 d, 0 and 0.5 Gy-exposed rats) after X-ray exposure, rats were euthanized by CO_2 asphyxiation, and the right testis and epididymis were removed for analysis as indicated above. Doses and time points for the X-ray experiment were based on previous studies of testis response to ionizing radiation (Hasegawa *et al.* 1997; Richburg *et al.* 2000; Yamasaki *et al.* 2010). Two p53−/− rats from the 0 Gy treatment group died before the study was completed, and were excluded from the analysis. One showed evidence of a tumor on the neck, while the other had no gross evidence of tumors. The timing of the deaths, 18 and 22 d after dosing, or PND 73–81, was coincident with the initial decrease in the survival curve for this model reported by McCoy *et al.* (2013).

Immunohistochemistry and Histological Analysis

Fixed testis tissue samples were processed through graded ethanols and embedded in paraffin. All paraffin sections for histology and immunohistochemistry were cut at 5 μm thickness. For routine histological analysis, slides were stained with hematoxylin and eosin (H&E). TUNEL staining was performed on formalin- or modified Davidson's-fixed and paraffin-embedded testis using the ApopTag Peroxidase In Situ Apoptosis Detection Kit (Millipore, Billerica, MA), with methyl green counterstain. Cleaved caspase-3 staining was performed using the SignalStain Apoptosis (Cleaved Caspase-3) IHC Detection Kit (Cell Signaling Technology, Danvers, MA), with hematoxylin counterstain. Identification of spermatogonial stem cells (SSCs) and calculation of SSC proliferation rate was performed using a modification of our previously reported serial sectioning procedure (Allard *et al.* 1995). Eleven 5 μm serial sections were obtained from modified Davidson's-fixed and paraffin-embedded testis. The middle section was stained with monoclonal mouse anti-BrdU clone Bu20a (#M0744; Dako, Carpinteria, CA) using our previously reported labeling protocol (Spade *et al.* 2015), which utilizes an HCl-mediated antigen retrieval procedure (Bak & Panos 1997). The outer sections were stained with H&E. SSCs were defined as isolated germ cells on the basement membrane, at least 25 μm away from any other germ cells, consistent with our previous work (Allard *et al.* 1995; Allard & Boekelheide 1996; Blanchard *et al.* 1996), and based on the definition of spermatogonial stem cells determined by studies of spermatogonia kinetics (Huckins 1971a; b; c). The SSC proliferative index was defined as the percentage of SSCs that stained positively for BrdU.

H&E-, TUNEL-, cleaved caspase-3- and BrdU-stained slides were scanned using an Aperio ScanScope CS (Leica Biosystems, Inc., Buffalo Grove, IL). Histology and apoptosis were analyzed by a treatment- and genotype-blind investigator on scanned slides using Leica ImageScope software. For each slide analyzed, a grid was used to select at least 50 effectively round seminiferous tubules, in which the length of the major axis was at most 1.5 times that of the minor axis. On H&E-stained slides, each selected seminiferous tubule was scored for atrophy, defined as a lack of germ cells along a significant portion of the seminiferous epithelium, germ cell sloughing (cellular material other than elongate spermatids present in the lumen), and presence of large vacuoles (greater than approximately 30 μm in greatest diameter and located on or near the seminiferous tubule basement

membrane), similar to our previously reported methods (Moffit *et al.* 2007). Minor axis seminiferous tubule diameter was also recorded for each tubule in the analysis. TUNEL-stained slides were scored for the presence of TUNEL-positive germ cells in tubules selected using a grid as in the H&E samples. However, all atrophic tubules were excluded. If fewer than 25 tubules remained after exclusion of atrophic tubules, all non-atrophic tubules in the section were scored. TUNEL data were analyzed as the proportion of scored tubules with 0, 1–3, and >3 TUNEL-positive germ cells. Cleaved caspase-3 slides were analyzed for pattern of expression by identifying all tubules with rosettes of cleaved caspase-3-positive spermatocytes and assigning the appropriate range of stages of spermatogenesis.

Immunofluorescence was used to qualitatively assess the localization of phosphorylated histone H2AX (γH2AX) in paraffin-embedded testis sections from p53+/+ and non-atrophic p53−/− rat testes. Sections were deparaffinized in xylene and rehydrated through a series of graded ethanols. Antigens were unmasked in 10 mM citrate buffer, pH 6.0, in a vegetable steamer for 20 m, followed by 20 m of cooling at room temperature. Tissue sections were blocked in a buffer consisting of 10% goat serum and 1% bovine serum albumin for 60 m at room temperature. Sections were incubated with monoclonal rabbit-anti-γH2AX antibody (Novus Biologicals, #NB100-79967), diluted 1:500 in blocking buffer, or blocking buffer alone as negative control, overnight at 4°C. The following day, sections were incubated with Alexa Fluor 647-conjugated goat-anti-rabbit IgG heavy and light chain secondary antibody (Life Technologies #A-21245) for 2 h at room temperature. Sections were counterstained with Hoechst 33342 (#62249, Thermo-Fisher Scientific, Waltham, MA) diluted 1:2000 in PBS for 1 h at room temperature and mounted with Molecular Probes Prolong Gold mounting medium (Thermo-Fisher Scientific). Throughout the staining procedure, all washes were performed with PBS. Confocal images were obtained on a Zeiss LSM 710 confocal microscope (Carl Zeiss Microscopy, Oberkochen, Germany).

GFRA1 staining was performed on paraformaldehyde-fixed seminiferous tubules to label type A spermatogonia. In the rat, GFRA1 labels A spermatogonia chains as long as $A_{al\text{-}32}$ (Marcon *et al.* 2011). Following fixation, seminiferous tubules were gently dispersed, mounted on glass slides, and then stained by immunofluorescence for GFRA1 and counterstained with DAPI using the method described by Lovasco *et al.* (2015). Tubules were washed with PBS 3 times, incubated in 0.1% Triton X-100 for 5 minutes, and then blocked with 0.05% Tween-20, 0.3 M glycine, 5% rabbit serum, and 1% bovine serum albumin (BSA) in PBS for 1 hour. Samples were incubated in polyclonal goat anti-GFRA1 primary antibody (#AF560; R&D Systems, Pittsburgh, PA), diluted 1:200 in PBS with 0.05% Tween-20 (PBST), or with PBST only as negative control, at 4°C overnight, then Alexa Fluor 488 donkey anti-goat IgG (H+L) secondary antibody (#A-11055; Life Technologies, Bedford, MA), diluted 1:500 in PBST, at room temperature for 2 hours. Rinses were performed with PBS between incubations. Finally, tubules were incubated in 100 ng/mL DAPI (Life Technologies, Bedford, MA), rinsed with PBS, and then mounted on glass slides using VECTASHIELD HardSet Mounting Medium (Vector Laboratories, Burlingame, CA). One highly atrophic p53 knockout rat testis could not be included in this analysis due to a lack of obvious GFRA1-positive clusters. We were also unable to include two other samples in the blind analysis leaving n = 3 p53 knockout and 4 wild-type samples. A minimum of 160 clusters and an average of 943.6 clusters were counted per sample. The

number of A_s, A_{pr}, $A_{al–4}$, $A_{al–8}$, and $A_{al–16}$ spermatogonial chains were counted using a Zeiss Axiovert 35 fluorescent microscope (Carl Zeiss AG, Oberkochen, Germany). Images were acquired on a Zeiss Axio Imager M1 fluorescent microscope.

Western Blots

γH2AX protein levels were quantified by Western blot according to previously published methods (Vantangoli *et al.* 2015). Briefly, frozen tissue samples were lysed in radioimmunoprecipitation assay (RIPA) buffer with HALT protease and phosphatase inhibitor (Thermo-Fisher Scientific). Total protein was quantified using the DC Protein Assay (Bio-Rad, Hercules, CA). 15 μg of protein per sample was separated by SDS-PAGE at 50 V for 2.25 h. Proteins were transferred to a PVDF membrane and blocked with 5% bovine serum albumin in TBS with 0.1% Tween-20. The membrane was stained for γH2AX and GAPDH, and each band was developed using Pierce ECL Western Blotting Substrate (Thermo-Fisher Scientific). Bands were quantified in Image J using the densitometry method of Gassman et al. (2009). Monoclonal rabbit-anti-γH2AX (Novus Biologicals, #NB100-79976) and monoclonal rabbit-anti-human GAPDH antibodies (Cell Signaling Technology, #2118) were each used at a 1:2000 dilution. For both proteins, the secondary antibody was goat-anti-rabbit IgG, HRP conjugate (Millipore, #12-348), diluted 1:2000.

Statistics

All data analysis was performed using Prism 6.07 (GraphPad Software, Inc., La Jolla, CA). Mean and standard error of the mean (SEM) are reported in figures. For most analyses, a two-sample hypothesis test was performed: data were checked for normality using the Komolgorov-Smirnov test, and differences between p53+/+ and p53−/− groups were analyzed using either the parametric two-tailed Student's t-test if data were normally distributed or the non-parametric Mann-Whitney U-test if data were non-normally distributed, as indicated in the figure legends. In figures 4, 7, and 8, multiple t-tests were performed in parallel, using the Holm-Sidak multiple test correction to test for significance at $\alpha = 0.05$. Testis atrophy data in figure 8K were analyzed by two-way ANOVA on the factors left/right testis (paired) and genotype (p53+/+ vs. p53−/−).

Results

Testicular atrophy in p53 knockout rats

On postnatal day 73 or 77, p53 knockout rats had a slightly lower average body weight and significantly lower testis and epididymis weights, compared to the wild-type (Fig. 1). In histological analysis of H&E-stained rat testis cross sections, some knockout animals exhibited widespread seminiferous tubule atrophy and abnormal testicular histopathology (Fig. 2). Atrophic tubules contained Sertoli cells and spermatogonia, but were significantly or completely depleted of spermatocytes and spermatids (Fig. 2B). 3 out of 5 p53 knockout rats had 50% or greater seminiferous tubule atrophy, while the remaining two had low rates of seminiferous tubule atrophy (Fig. 2E). In contrast to the p53 knockout rats, seminiferous tubule atrophy was infrequent in the wild-type rat testes. We also observed a significantly elevated frequency of large vacuoles in p53 knockout seminiferous tubules; however, large vacuoles were relatively rare, as only 15 were identified in a total of 573 scored tubules, five

of which were in atrophic tubules (Fig. 2F). Germ cell sloughing was not significantly elevated in p53 knockout rats (Fig. 2G). When considering all categories of abnormalities scored in the study together, the proportion of tubules with any abnormality was significantly higher in p53 knockout than wild-type rat testes (Fig. 2H). p53 knockout testes also had smaller seminiferous tubule diameters than wild-type testes, with fewer visible elongate spermatids preparing to release in histological sections of stage VII-VIII tubules (Fig. 3).

Germ cell death is elevated in p53 knockout testes

Germ cell death was quantified by measuring the percentage of seminiferous tubules per testis that contained 0, 1–3, or >3 TUNEL-labeled cells. p53 knockout rats exhibited significantly increased levels of germ cell death compared to the wild-type, with significantly fewer tubules exhibiting 0 TUNEL-positive germ cells, and significantly greater proportions of tubules with 1–3 and >3 TUNEL-positive germ cells (Fig. 4A). p53 knockout rats also had a greater overall frequency of TUNEL-positive germ cells (Fig. 4B) and TUNEL-positive spermatogonia (Fig. 4C). However, the proportion of TUNEL-positive cells that were identified as spermatogonia trended slightly higher in p53+/+ than p53−/− testes (Fig. 4D). In wild-type testes, TUNEL staining was infrequent, mostly consisting of TUNEL-positive spermatogonia in stages I–VI and XII–XIV (Fig. 4E–H). However, in the p53 knockout testis, widespread TUNEL staining was observed, particularly in spermatocytes, in all stages except for IX-XI, predominantly in stages I–VI and XII–XIV (Fig. 4I–L). While TUNEL staining was present in both normal and atrophic knockout seminiferous tubules, a large number of atrophic tubules in p53−/− rats contained no TUNEL-positive cells because they contained very few germ cells of any kind. Consequently, atrophic tubules were excluded from this analysis.

Cleaved caspase-3 staining was observed in both p53 knockout and wild-type rats (Fig. 5). However, it did not correspond directly to the pattern of TUNEL staining. Cleaved caspase-3 was present in the cytoplasm and perinuclear region of spermatids, most prominently in stages VII–VIII. The staining was more intense in some tubules in p53 knockout testes than wild-type.

Comparison of H2AX phosphorylation between p53 knockout and wild-type rats

To assess the hypothesis that germ cell death in p53 knockout rats is preceded by accumulation of DNA double-strand breaks in p53 knockout rats, we quantified phosphorylated histone H2AX (γH2AX) by Western blot and localized γH2AX by immunofluorescence. Western blot analysis of γH2AX indicated that there was no significant difference between wild-type and p53 knockout rat testis (Fig. 6A). While the average γH2AX protein level was slightly lower in the p53 knockout than wild-type rats, it was decreased in the three mostly atrophic samples and normal in the testes with low levels of atrophy. Qualitative immunofluorescent analysis of γH2AX showed no obvious variation in staining patterns between genotypes (Fig. 6B–K). In both wild-type and p53-knockout testis tubules, γH2AX labeling was observed in the sex vesicles of pachytene spermatocytes throughout multiple stages. A large number of γH2AX foci were present in leptotene spermatocytes in stages IX-XI (Fig. 6F, I). The number of foci decreased slightly in

zygotene spermatocytes in stages XII–XIII (Fig. 6G, J), and condensed further into the sex vesicles in early pachytene spermatocytes by stage XIV (Fig. 6H, K).

Normal spermatogonial stem cell proliferation and undifferentiated spermatogonia population in p53 knockout rats

Seminiferous tubules were examined for both the total quantity of undifferentiated type A spermatogonia and also the percentage of each type of spermatogonial cluster (A_s, A_{pr}, $A_{al–4}$, $A_{al–8}$, and $A_{al–16}$) relative to the total (Fig. 7A). There was no significant difference between the knockout and the wild-type seminiferous tubules in the total number of clusters per mm (Fig. 7B) or in the proportion of chain lengths present (Fig. 7C). This indicated that the undifferentiated spermatogonia population, and by extension the pattern of undifferentiated spermatogonial proliferation, was normal in the knockout rats and was unaffected by the lack of p53, though the most atrophic samples could not be counted.

Spermatogonial stem cells (SSCs), defined as germ cells basally positioned on the basement membrane that are at least 25 μm away from any other germ cell, were identified in serial histological sections of germ cell-depleted testes. Two p53 knockout testes in this study had enough atrophic tubules to allow for identification and characterization of SSCs following our previously reported method (Allard *et al.* 1995) (Figure S1). The SSC proliferative index, defined as the proportion of SSCs that stained positively for BrdU, was 0.375 and 0.368 in these atrophic testes (Table 1), similar to the approximately 40% SSC proliferation rate observed with 14-day BrdU exposure seven weeks after germ cell depletion by 2,5-hexanedione (Allard *et al.* 1995). Therefore, it appears that atrophic p53 knockout rats retain the capacity to regenerate spermatogonia from the SSC population.

Germ cell response to X-radiation in p53-knockout rats

In histopathological analysis of 0.5 and 5 Gy-exposed rats analyzed 3 h after irradiation, the rate of atrophy was higher in p53 knockout than wild-type rats, with at least one significant comparison between genotypes in the 0, 1–3, and >3 TUNEL-positive cell measures, (Fig. 8A–B), consistent with our analysis of unirradiated p53 knockout testes. However, 12 h after X-ray exposure, 5 Gy-irradiated testes of wild-type rats had elevated germ cell TUNEL labeling rates that were not significantly different from the p53 knockout animals (Fig. 8C), indicating that acute high-dose X-ray exposure causes a similar frequency of germ cell death to that which occurs spontaneously in p53 knockout rat testes. The pattern of TUNEL-positive cells differed between wild-type and p53 knockout testes, however. TUNEL-positive spermatogonia were visible in both genotypes following X-radiation, but TUNEL-positive spermatocytes were much more commonly observed in p53 knockout testes (Fig. 8D). As a result, the proportion of TUNEL-positive germ cells that were identified as spermatogonia was higher in wild-type than p53 knockout testes (Fig. 8E–G). As in Figure 4, atrophic tubules were excluded from this analysis. Also consistent with the unirradiated animals, 6 weeks after X-ray exposure, p53 knockout rat body weights trended lower, but were not significantly different from wild-type (Fig. 8H). Testis and epididymis weights were significantly lower in both irradiated and non-irradiated p53 knockout rats compared to wild-type (Fig. 8I, J). Consistent with reduced testis weight, while the rate of seminiferous tubule atrophy was uniformly near zero in wild-type rat testes, it was variable in p53

knockout rats, regardless of dose and time point, with 11 out of 30 samples having greater than 30% atrophic tubules (Fig. 8K).

Discussion

Elevated germ cell death leads to spontaneous atrophy of p53 knockout rat testes

The p53 knockout rat exhibited spontaneous seminiferous tubule atrophy characterized by a loss of testis weight and germ cell depletion (Figs. 1–3). Especially in p53 knockout rats with low rates of atrophy, spermatocyte TUNEL frequency was elevated (Fig. 4), which indicates that atrophy likely occurs following large scale loss of germ cells, particularly spermatocytes. BrdU and GFRA1 analyses verified that SSC proliferation and the undifferentiated spermatogonia population were normal in the knockout animals, and that the breakdown occurred in later stages of spermatogenesis (Figs. 6–7, Table 1). Experiments with X-ray exposure in p53 knockout rats confirmed that seminiferous tubule atrophy occurred spontaneously across a larger sample size, and also that the rate of germ cell apoptosis in p53 knockout rats was similar to the rate observed 12 h after a high dose of radiation in wild-type rats. However, X-ray exposure caused primarily spermatogonia loss, while p53 knockout rat germ cell loss primarily affected the spermatocytes (Fig. 8). Widespread apoptotic germ cell loss observed in non-irradiated p53 knockout rats mimics the effects of classic germ cell toxicants, such as X-radiation. While high dose exposures to Sertoli cell toxicants such as 2,5-hexanedione also lead to germ cell apoptosis (Allard & Boekelheide 1996; Blanchard *et al.* 1996; Moffit *et al.* 2007), ionizing radiation leads to a sharp increase in germ cell apoptosis peaking at approximately 12 h after exposure (Hasegawa *et al.* 1997; Richburg *et al.* 2000), and in particular leads to greater numbers of apoptotic germ cells than HD exposure (Moffit *et al.* 2007). Paradoxically, while the baseline rate of germ cell death in p53 knockout rat testis is high, high-dose ionizing radiation fails to elevate it further, indicating that the p53 knockout rat, much like p53-deficient mouse models, may be protected from p53-dependent radiation-induced apoptosis. This could be the result of X-ray exposure targeting spermatogonia while p53 knockout testis germ cell loss is largely limited to spermatocytes. While the intensity of cleaved caspase-3 signal was greater in the spermatocytes of p53-knockout than wild-type rats (Fig. 4), the pattern of localization did not correspond with TUNEL, which appears to indicate that the process leading to germ cell death in p53-knockout rats is not dependent on activation of caspase-3.

Based on the pattern of TUNEL staining, the block in spermatogenesis appeared to occur during meiotic prophase I in leptotene and zygotene spermatocytes. p53 has a known role in homologous recombination. The first step of homologous recombination is the introduction of a double strand break (DSB) in the DNA, a process that is initiated by the topoisomerase SPO11 in leptotene spermatocytes, in a fashion that is conserved across species (Mahadevaiah *et al.* 2001; Chicheportiche *et al.* 2007; Blanco-Rodriguez 2009; Lu *et al.* 2010). p53 is activated by SPO11-induced DSBs and subsequently recruits DNA repair proteins including RAD51 and DMC1 to repair the DSB by recombination (Habu *et al.* 2004; Gatz & Wiesmuller 2006; Lu *et al.* 2010). Loss of p53 could render spermatocytes unable to resolve the DSB, leading to an accumulation of DSBs, which would initiate apoptotic death. We tested this hypothesis by analyzing phosphorylation of histone H2AX in

the rat testis both by Western blot and immunofluorescence. H2AX is a histone that is phosphorylated (denoted γH2AX) in both DSB-dependent and -independent manners during meiotic recombination (Hamer *et al.* 2003; Blanco-Rodriguez 2012). γH2AX distribution was similar in the non-atrophic seminiferous tubules of p53 knockout and wild-type rats. It has been reported that X-radiation causes an increase in γH2AX foci, but not quantity of γH2AX protein according to Western blot, in mouse and rat testes (Hamer *et al.* 2003; Ishizaki *et al.* 2004; Mah *et al.* 2010).

In p53-knockout rat testes we did not see evidence of a significant difference in the quantity of γH2AX protein between genotypes. However, we observed that the lowest γH2AX protein levels in our analysis came from testes with high rates of apoptotic tubules (Fig. 6A). We also did not find evidence of increased γH2AX foci in the p53 knockouts by immunofluorescence. However, the pattern of γH2AX expression is consistent with the creation of DSBs in leptotene and zygotene spermatocytes prior to synapsis (Fig. 6). The creation of DSBs by SPO11 in leptotene and zygotene spermatocytes corresponds with the γH2AX foci we observed in tubules of stages IX-XI and XII–XIV. Failure to resolve these DSBs could explain increased rates of spermatocyte death observed in p53-knockout testes in some tubules of stage XII–XIV and I–VI (Fig. 4). The apoptotic spermatocytes in those stage ranges are zygotene/pachytene spermatocytes in stages XII–XIV and pachytene spermatocytes in stages I–VI, derived from the leptotene and zygotene pachytene cells, respectively, in which γH2AX labeling was observed. This observation is consistent with the hypothesis that elevated double strand breaks in p53-knockout mouse zygotene and leptotene spermatocytes lead to the loss of spermatocytes in stages XII–XIV and I–VI. However, this hypothesis requires further quantitative testing in future studies.

p53 knockout rats also had lower testis and epididymis weights than wild-type rats (Figs. 1 and 8). These effects were consistent across all p53 knockout rats, not confined to the rats with high rates of seminiferous tubule atrophy. Consistent with these findings, p53 knockout rats had lower mean seminiferous tubule diameter and qualitatively reduced numbers of elongate spermatids preparing to release in stages VII–VIII of spermatogenesis (Fig. 3). Reduced germ cell throughput in spermatogenesis would explain reduced epididymal weight and decreased seminiferous tubule diameter in non-atrophic p53 knockout testes (Vidal & Whitney 2014). Therefore, p53 knockout rat testes show evidence of reduced spermatogenesis, even in tubules that are not atrophic.

The undifferentiated spermatogonia population is normal in atrophic p53 knockout rat testes

Spermatogonial stem cells (SSCs), a subclass of type A spermatogonia, are the progenitor cells of spermatogenesis. SSCs give rise through mitotic division to single type A spermatogonia (A_s), which divide to form pairs (A_{pr}) and subsequently longer chains of aligned spermatogonia ($A_{al–4}$, $A_{al–8}$, and $A_{al–16}$) (Huckins 1971a). GDNF family receptor alpha 1 (GFRA1) is a germ cell surface receptor that functions in spermatogonial self-renewal and proliferation. It is selectively expressed by undifferentiated type A spermatogonia (Grisanti *et al.* 2009). It has previously been demonstrated that a combination of bleomycin, cisplatin, and etoposide reduces the number of type A spermatogonial clusters

present in rat seminiferous tubules, while increasing the proportion of A_s and A_{pr} clusters relative to longer chains (Marcon *et al.* 2011). Conversely, mice lacking Taf4b have a decreased proportion of A_s and increased $A_{al–8}$ and $A_{al–16}$ clusters (Lovasco *et al.* 2015). If spermatogonial proliferation was altered in p53 knockout rats, we expected to see a change in the distribution of type A spermatogonia favoring shorter cluster sizes in p53 knockout rat seminiferous tubules. However, we saw no such difference (Fig. 7). Our results indicated that non-atrophic p53 knockout testes are not impaired in their capacity for type A spermatogonial proliferation.

The SSC population is renewed through the separation of A_{pr} spermatogonia back into isolated A_s SSCs. SSCs tend to be resistant to exposures such as 2,5-hexanedione and X-radiation that cause germ cell death (Allard *et al.* 1995; Hasegawa *et al.* 1998). After germ cell depletion, if a viable A_s SSC population remains, the testis retains the capacity for germ cell self-renewal. We investigated the self-renewal potential of the most atrophic p53 knockout rats in this study by analyzing the BrdU labeling rate of SSCs after a long-term BrdC exposure. Upon its uptake into cells, BrdC is de-aminated to form BrdU, which is then incorporated during S-phase DNA replication and can be used to label actively proliferating cells (Conner *et al.* 1978). In a previous study of rats exposed to 2,5-hexanedione to deplete the germ cell population, the proliferative index of SSCs was found to be approximately 0.4 after 13 days of BrdC exposure (Allard *et al.* 1995). In the present study, proliferation rates for SSCs in the two most atrophic p53 knockout rat testes were 0.375 and 0.368 (Table 1). The presence of proliferative spermatogonial stem cells in the p53 knockout rat testis indicates that atrophic tubules in the testes of p53 knockout rats assessed in this study retained the capacity to repopulate their atrophic seminiferous tubules. This is consistent with mouse data indicating that radiation-induced SSC apoptosis is p53-dependent (Coureuil *et al.* 2010; Ishii *et al.* 2014). That SSC proliferation and the undifferentiated spermatogonia population were normal in the knockout animals was consistent with the block in spermatogenesis occurring later in the spermatogenesis, associated with DNA double-strand breaks generated in spermatocytes.

The role of p53 in spermatogenesis

p53 is known to have a significant role in spermatogenesis, based on studies of p53-knockout mice, and our present report confirms that this is also true in the rat. However, the apparent role of p53 in spermatogenesis differs across studies of p53 mutant mice. On one hand, several studies report apparently germ cell protective effects of p53 loss, including elevated numbers of type A spermatogonia and reduced apoptotic response to X-radiation (Beumer *et al.* 1998), as well as increased average testis weight of p53 knockout mice on a C57 background relative to wild-type (Golas *et al.* 2011), suggesting that germ cells accumulate abnormally in p53 knockout mice. Induction of apoptosis via upregulation of *Fas* in response to X-radiation is inhibited in the testes of p53 knockout mice (Hasegawa *et al.* 1998; Embree-Ku *et al.* 2002), which could explain abnormal germ cell accumulation.

Conversely, despite the role of p53 in normal germ cell apoptosis, some studies have indicated that the testes of p53 deficient mice are prone to spontaneous degeneration (Rotter *et al.* 1993; Golas *et al.* 2011). Unlike the results of the present study, in which p53 knockout

rats retained a normal spermatogonial population and SSC proliferation rate, it has been reported that the seminiferous tubules of p53 knockout mice recover more slowly than wild-type mice following very high doses of radiation (Hendry *et al.* 1996). Similar to the present study, p53 heterozygotes and knockouts have been shown to have higher rates of DNA double-strand breaks in pachytene spermatocytes and apoptotic germ cells (Paul *et al.* 2007). Therefore, depending on the model background and study conditions, p53 loss may result in either germ cell protective effects or enhanced germ cell loss.

p53 is expressed in testicular germ cells, primarily in spermatocytes (Sjoblom & Lahdetie 1996; Hu 2009). Because p53 is required for meiotic recombination, loss of germ cell DNA integrity in the absence of p53 would explain the altered germ cell dynamics observed in p53 mutant model studies. Therefore, p53 has a role in promoting germ cell apoptosis in certain conditions, but the lack of p53 also leads to germ cell loss in some models, apparently resulting from failure to resolve DSBs in meiosis. In mice, the precise implications of p53 loss for spermatogenesis depend on the genetic background, which indicates that p53 has multiple roles in germ cell survival, meiosis, and differentiation. Our results indicate that p53 is similarly important for spermatogenesis in the rat, though the histopathological outcome differs from that which has been observed in mice.

It is notable that p53 deficient model rodents are fertile despite the adverse effects of p53 loss on spermatogenesis. In fact, in the p53 knockout rat model used in the present study, germ cell death and seminiferous tubule atrophy rates were variable (Figs. 2 and 4), and p53−/− males of this strain can be bred successfully with wild-type females (McCoy *et al.* 2013). p53 knockout mice of C57BL/6 background have significantly reduced pregnancy rate and litter size only when using p53−/− female mice, not p53−/− males alone. However, in both C57BL/6 and 129SV-derived strains, the effect of p53 loss on reproduction is greatest when male p53−/− and female p53−/− animals are bred (Hu *et al.* 2007). Taken together, the evidence indicates that male p53 knockout rats and mice have dysfunctions in spermatogenesis that are likely to lead to subfertility. These findings have important implications for the role of p53 in human spermatogenesis. Notably, as in the mouse, genetic background is likely to influence the effects of p53 loss in the rat testis. Therefore, additional comparisons between this model and the models generated by different methods of mutagenesis on Wistar or Dark Agouti/F344/Sprague Dawley backgrounds (Tong *et al.* 2010; van Boxtel *et al.* 2011) would be appropriate for future studies.

The results of the present study indicate that p53 plays a significant role in rat spermatogenesis, as it does in the mouse, but with variable and complex disruptive effects. We have shown that zygotene and pachytene spermatocytes in stages XII–XIV and I–VI, respectively, undergo spontaneous cell death leading to seminiferous tubule atrophy in the p53 knockout rat testis, while SSC proliferation and the type A spermatogonia population are unaffected. Future studies should be conducted to further clarify the p53-independent molecular mechanisms of germ cell death in p53 knockout rats including quantification of spermatocyte DNA damage, as well as the evolution of the testicular atrophy in p53 knockout rats following repeated breeding.

Supplementary Material

Refer to Web version on PubMed Central for supplementary material.

Acknowledgments

Funding Information

This study was funded by the National Institute of Environmental Health Sciences (R01ES017272 to KB, T32ES007272 support to DS, K99ES025231 to DS).

The authors thank Dr. Richard Freiman's laboratory for generously providing advice and microscope use for this project. We thank Melinda Golde for processing of samples for histology and Shelby Wilson for assistance with TUNEL scoring.

References

Allard EK, Boekelheide K. Fate of germ cells in 2,5-hexanedione-induced testicular injury. II. Atrophy persists due to a reduced stem cell mass and ongoing apoptosis. Toxicol Appl Pharmacol. 1996; 137:149–156. [PubMed: 8848794]

Allard EK, Hall SJ, Boekelheide K. Stem cell kinetics in rat testis after irreversible injury induced by 2,5-hexanedione. Biol Reprod. 1995; 53:186–192. [PubMed: 7669848]

Bak PM, Panos RJ. Protease antigen recovery decreases the specificity of bromodeoxyuridine detection in formalin-fixed tissue. J Histochem Cytochem. 1997; 45:1165–1170. [PubMed: 9267477]

Benchimol S. p53-dependent pathways of apoptosis. Cell Death Differ. 2001; 8:1049–1051. [PubMed: 11687883]

Beumer TL, Roepers-Gajadien HL, Gademan IS, van Buul PP, Gil-Gomez G, Rutgers DH, de Rooij DG. The role of the tumor suppressor p53 in spermatogenesis. Cell Death Differ. 1998; 5:669–677. [PubMed: 10200522]

Blanchard KT, Allard EK, Boekelheide K. Fate of germ cells in 2,5-hexanedione-induced testicular injury. I. Apoptosis is the mechanism of germ cell death. Toxicol Appl Pharmacol. 1996; 137:141–148. [PubMed: 8661338]

Blanco-Rodriguez J. gammaH2AX marks the main events of the spermatogenic process. Microsc Res Tech. 2009; 72:823–832. [PubMed: 19405149]

Blanco-Rodriguez J. Programmed phosphorylation of histone H2AX precedes a phase of DNA double-strand break-independent synapsis in mouse meiosis. Reproduction. 2012; 144:699–712. [PubMed: 23035256]

Chicheportiche A, Bernardino-Sgherri J, de Massy B, Dutrillaux B. Characterization of Spo11-dependent and independent phospho-H2AX foci during meiotic prophase I in the male mouse. J Cell Sci. 2007; 120:1733–1742. [PubMed: 17456548]

Conner MK, Boggs SS, Turner JH. Comparisons of in vivo BrdU labeling methods and spontaneous sister chromatid exchange frequencies in regenerating murine liver and bone marrow cells. Chromosoma. 1978; 68:303–311. [PubMed: 81738]

Coureuil M, Ugolin N, Tavernier M, Chevillard S, Barroca V, Fouchet P, Allemand I. Puma and Trail/Dr5 pathways control radiation-induced apoptosis in distinct populations of testicular progenitors. PLoS One. 2010; 5:e12134. [PubMed: 20711434]

Embree-Ku M, Venturini D, Boekelheide K. Fas is involved in the p53-dependent apoptotic response to ionizing radiation in mouse testis. Biol Reprod. 2002; 66:1456–1461. [PubMed: 11967210]

Fouchecourt S, Livera G, Messiaen S, Fumel B, Parent AS, Marine JC, Monget P. Apoptosis of Sertoli cells after conditional ablation of murine double minute 2 (Mdm2) gene is p53-dependent and results in male sterility. Cell Death Differ. 2016; 23:521–530. [PubMed: 26470726]

Fridman JS, Lowe SW. Control of apoptosis by p53. Oncogene. 2003; 22:9030–9040. [PubMed: 14663481]

Gassmann M, Grenacher B, Rohde B, Vogel J. Quantifying Western blots: pitfalls of densitometry. Electrophoresis. 2009; 30:1845–1855. [PubMed: 19517440]

Gatz SA, Wiesmuller L. p53 in recombination and repair. Cell Death Differ. 2006; 13:1003–1016. [PubMed: 16543940]

Golas A, Lech T, Janula M, Bederska D, Lenartowicz M, Styrna J. Semen quality parameters and embryo lethality in mice deficient for Trp53 protein. Reprod Biol. 2011; 11:250–263. [PubMed: 22139338]

Grisanti L, Falciatori I, Grasso M, Dovere L, Fera S, Muciaccia B, Fuso A, Berno V, Boitani C, Stefanini M, Vicini E. Identification of spermatogonial stem cell subsets by morphological analysis and prospective isolation. Stem Cells. 2009; 27:3043–3052. [PubMed: 19711452]

Habu T, Wakabayashi N, Yoshida K, Yomogida K, Nishimune Y, Morita T. p53 Protein interacts specifically with the meiosis-specific mammalian RecA-like protein DMC1 in meiosis. Carcinogenesis. 2004; 25:889–893. [PubMed: 14764457]

Hamer G, Roepers-Gajadien HL, van Duyn-Goedhart A, Gademan IS, Kal HB, van Buul PP, de Rooij DG. DNA double-strand breaks and gamma-H2AX signaling in the testis. Biol Reprod. 2003; 68:628–634. [PubMed: 12533428]

Hasegawa M, Wilson G, Russell LD, Meistrich ML. Radiation-induced cell death in the mouse testis: relationship to apoptosis. Radiat Res. 1997; 147:457–467. [PubMed: 9092926]

Hasegawa M, Zhang Y, Niibe H, Terry NH, Meistrich ML. Resistance of differentiating spermatogonia to radiation-induced apoptosis and loss in p53-deficient mice. Radiat Res. 1998; 149:263–270. [PubMed: 9496889]

Hendry JH, Adeeko A, Potten CS, Morris ID. P53 deficiency produces fewer regenerating spermatogenic tubules after irradiation. Int J Radiat Biol. 1996; 70:677–682. [PubMed: 8980665]

Hollstein M, Sidransky D, Vogelstein B, Harris CC. p53 mutations in human cancers. Science. 1991; 253:49–53. [PubMed: 1905840]

Hu W. The role of p53 gene family in reproduction. Cold Spring Harb Perspect Biol. 2009; 1:a001073. [PubMed: 20457559]

Hu W, Feng Z, Teresky AK, Levine AJ. p53 regulates maternal reproduction through LIF. Nature. 2007; 450:721–724. [PubMed: 18046411]

Huckins C. The spermatogonial stem cell population in adult rats. I. Their morphology, proliferation and maturation. Anat Rec. 1971a; 169:533–557. [PubMed: 5550532]

Huckins C. The spermatogonial stem cell population in adult rats. II. A radioautographic analysis of their cell cycle properties. Cell Tissue Kinet. 1971b; 4:313–334. [PubMed: 5127356]

Huckins C. The spermatogonial stem cell population in adult rats. III. Evidence for a long-cycling population. Cell Tissue Kinet. 1971c; 4:335–349. [PubMed: 5127357]

Ishii K, Ishiai M, Morimoto H, Kanatsu-Shinohara M, Niwa O, Takata M, Shinohara T. The Trp53-Trp53inp1-Tnfrsf10b pathway regulates the radiation response of mouse spermatogonial stem cells. Stem Cell Reports. 2014; 3:676–689. [PubMed: 25358794]

Ishizaki K, Hayashi Y, Nakamura H, Yasui Y, Komatsu K, Tachibana A. No induction of p53 phosphorylation and few focus formation of phosphorylated H2AX suggest efficient repair of DNA damage during chronic low-dose-rate irradiation in human cells. J Radiat Res. 2004; 45:521–525. [PubMed: 15635261]

Jacks T, Remington L, Williams BO, Schmitt EM, Halachmi S, Bronson RT, Weinberg RA. Tumor spectrum analysis in p53-mutant mice. Curr Biol. 1994; 4:1–7. [PubMed: 7922305]

Lovasco LA, Gustafson EA, Seymour KA, de Rooij DG, Freiman RN. TAF4b is required for mouse spermatogonial stem cell development. Stem Cells. 2015; 33:1267–1276. [PubMed: 25727968]

Lu WJ, Chapo J, Roig I, Abrams JM. Meiotic recombination provokes functional activation of the p53 regulatory network. Science. 2010; 328:1278–1281. [PubMed: 20522776]

Mah LJ, El-Osta A, Karagiannis TC. gammaH2AX: a sensitive molecular marker of DNA damage and repair. Leukemia. 2010; 24:679–686. [PubMed: 20130602]

Mahadevaiah SK, Turner JM, Baudat F, Rogakou EP, de Boer P, Blanco-Rodriguez J, Jasin M, Keeney S, Bonner WM, Burgoyne PS. Recombinational DNA double-strand breaks in mice precede synapsis. Nat Genet. 2001; 27:271–276. [PubMed: 11242108]

Malkin D. p53 and the Li-Fraumeni syndrome. Cancer Genet Cytogenet. 1993; 66:83–92. [PubMed: 8500106]

Malkin D, Li FP, Strong LC, Fraumeni JF Jr, Nelson CE, Kim DH, Kassel J, Gryka MA, Bischoff FZ, Tainsky MA, et al. Germ line p53 mutations in a familial syndrome of breast cancer, sarcomas, and other neoplasms. Science. 1990; 250:1233–1238. [PubMed: 1978757]

Marcon L, Zhang X, Hales BF, Robaire B, Nagano MC. Effects of chemotherapeutic agents for testicular cancer on rat spermatogonial stem/progenitor cells. J Androl. 2011; 32:432–443. [PubMed: 21088230]

McCoy A, Besch-Williford CL, Franklin CL, Weinstein EJ, Cui X. Creation and preliminary characterization of a Tp53 knockout rat. Dis Model Mech. 2013; 6:269–278. [PubMed: 22917926]

Moffit JS, Bryant BH, Hall SJ, Boekelheide K. Dose-dependent effects of sertoli cell toxicants 2,5-hexanedione, carbendazim, and mono-(2-ethylhexyl) phthalate in adult rat testis. Toxicol Pathol. 2007; 35:719–727. [PubMed: 17763286]

Paul C, Povey JE, Lawrence NJ, Selfridge J, Melton DW, Saunders PT. Deletion of genes implicated in protecting the integrity of male germ cells has differential effects on the incidence of DNA breaks and germ cell loss. PLoS One. 2007; 2:e989. [PubMed: 17912366]

Richburg JH, Nanez A, Williams LR, Embree ME, Boekelheide K. Sensitivity of testicular germ cells to toxicant-induced apoptosis in gld mice that express a nonfunctional form of Fas ligand. Endocrinology. 2000; 141:787–793. [PubMed: 10650961]

Rotter V, Schwartz D, Almon E, Goldfinger N, Kapon A, Meshorer A, Donehower LA, Levine AJ. Mice with reduced levels of p53 protein exhibit the testicular giant-cell degenerative syndrome. Proc Natl Acad Sci U S A. 1993; 90:9075–9079. [PubMed: 8415656]

Scherthan H, Jerratsch M, Dhar S, Wang YA, Goff SP, Pandita TK. Meiotic telomere distribution and Sertoli cell nuclear architecture are altered in Atm- and Atm-p53-deficient mice. Mol Cell Biol. 2000; 20:7773–7783. [PubMed: 11003672]

Schwartz D, Goldfinger N, Rotter V. Expression of p53 protein in spermatogenesis is confined to the tetraploid pachytene primary spermatocytes. Oncogene. 1993; 8:1487–1494. [PubMed: 8502474]

Sjoblom T, Lahdetie J. Expression of p53 in normal and gamma-irradiated rat testis suggests a role for p53 in meiotic recombination and repair. Oncogene. 1996; 12:2499–2505. [PubMed: 8700508]

Spade DJ, Hall SJ, Wilson S, Boekelheide K. Di-n-Butyl Phthalate Induces Multinucleated Germ Cells in the Rat Fetal Testis Through a Nonproliferative Mechanism. Biol Reprod. 2015; 93:110. [PubMed: 26400400]

Tong C, Li P, Wu NL, Yan Y, Ying QL. Production of p53 gene knockout rats by homologous recombination in embryonic stem cells. Nature. 2010; 467:211–213. [PubMed: 20703227]

van Boxtel R, Kuiper RV, Toonen PW, van Heesch S, Hermsen R, de Bruin A, Cuppen E. Homozygous and heterozygous p53 knockout rats develop metastasizing sarcomas with high frequency. Am J Pathol. 2011; 179:1616–1622. [PubMed: 21854749]

Vantangoli MM, Madnick SJ, Huse SM, Weston P, Boekelheide K. MCF-7 Human Breast Cancer Cells Form Differentiated Microtissues in Scaffold-Free Hydrogels. PLoS One. 2015; 10:e0135426. [PubMed: 26267486]

Venkatachalam S, Tyner SD, Pickering CR, Boley S, Recio L, French JE, Donehower LA. Is p53 haploinsufficient for tumor suppression? Implications for the p53+/− mouse model in carcinogenicity testing. Toxicol Pathol. 2001; 29(Suppl):147–154. [PubMed: 11695551]

Vidal JD, Whitney KM. Morphologic manifestations of testicular and epididymal toxicity. Spermatogenesis. 2014; 4:e979099. [PubMed: 26413388]

Yamasaki H, Sandrof MA, Boekelheide K. Suppression of radiation-induced testicular germ cell apoptosis by 2,5-hexanedione pretreatment. I. Histopathological analysis reveals stage dependence of attenuated apoptosis. Toxicol Sci. 2010; 117:449–456. [PubMed: 20616207]

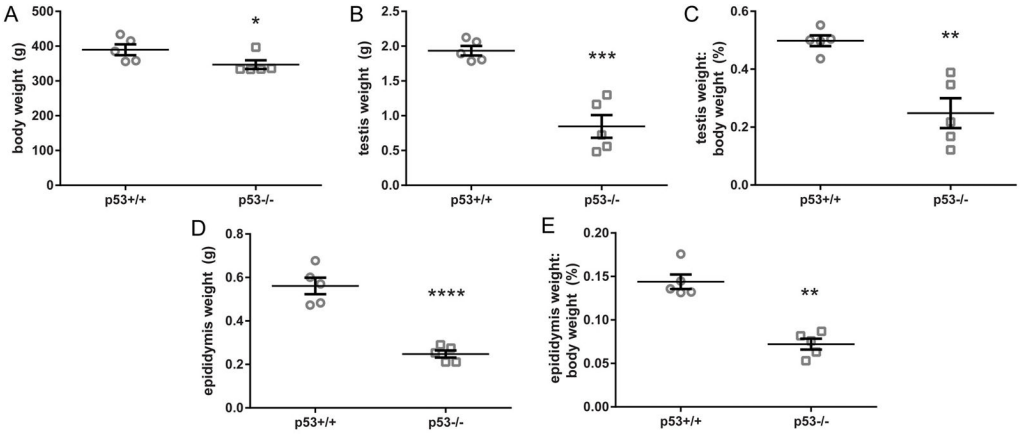

Figure 1.

Body and gross organ weights (mean ± SEM) on postnatal day 73 or 77. p53−/− rats have similar body weights (A), but significantly lower testis (B, C) and epididymis (D, E) weights, as well as organ:body weight ratios (C,E), compared to p53+/+. *$p < 0.05$; **$p < 0.01$; ***$p < 0.001$, ****$p < 0.0001$ by either two-tailed t-test (testis and epididymis weight) or Mann-Whitney U test (body weight) (n = 5 rats). Left and right testis and epididymis weights from each animal were averaged and the average was analyzed as a single biological replicate.

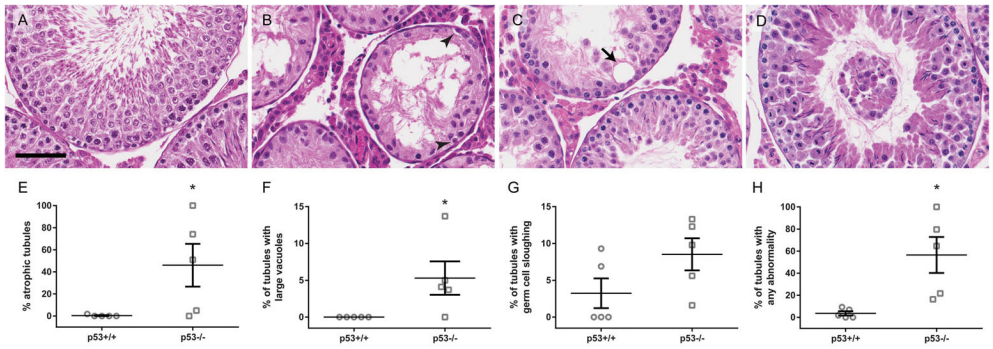

Figure 2.

p53−/− rats have higher rates of atrophy and other testicular pathology than p53+/+. p53+/+ and p53−/− rat testis sections were stained with H&E. Histological images show a normal seminiferous tubule in a p53+/+ testis (A), as well as examples of atrophy (B), a large vacuole (C, arrow), and germ cell sloughing (D) in p53−/− testes. Scale bar = 60 μm. Arrowheads in B identify spermatogonia in the atrophic tubule. p53−/− testes display significantly increased levels of seminiferous tubule atrophy (E) and large vacuoles (F), but not sloughing (G), compared to the wild-type. When all abnormalities were considered together, p53−/− rats also had a significantly higher rate than wild-type (H). Mean ± SEM reported in E–H. Scored 51–73 tubules per left testis from each animal (mean = 57.3 tubules). *$p < 0.05$ by the Mann-Whitney U test (atrophy, vacuoles, all) or t-test (sloughing) (n = 5 rats).

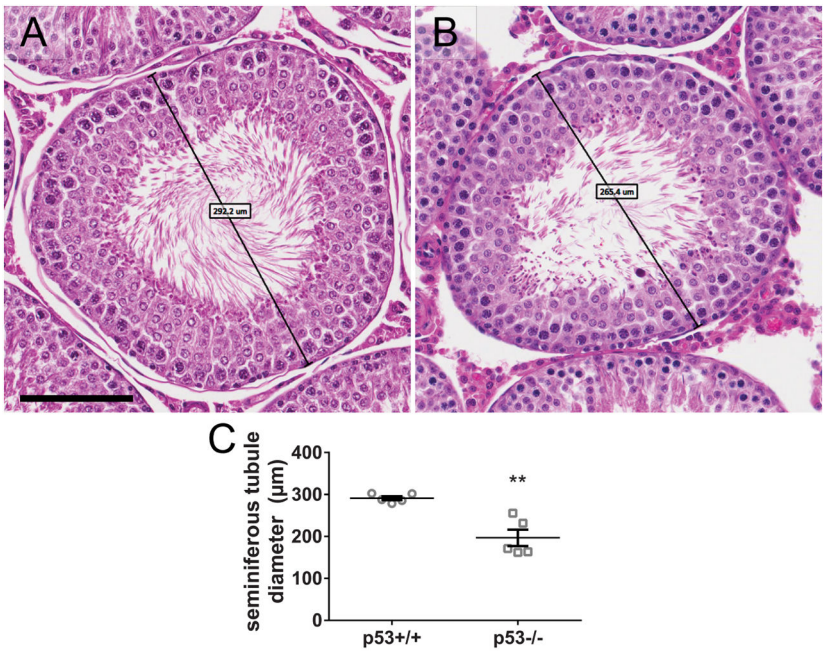

Figure 3.

p53−/− rats have reduced seminiferous tubule diameter and spermatid release, relative to p53+/+. Representative images of stage VII/VIII seminiferous tubules in a p53+/+ testis (A) and a p53−/− testis (B), showing reduced numbers of elongate spermatids releasing in p53−/− testes. Representative minor axis seminiferous tubule diameters measure 292.2 μm and 265.4 μm, respectively. Scale bar = 100 μm. Seminiferous tubule diameter was measured for 51–73 tubules (mean = 57.3 tubules) on H&E-stained left testis sections. The average tubule diameter (mean ± SEM) is lower in p53−/− testes than p53+/+, including both atrophic and normal p53−/− samples (C). $^{**}p < 0.01$ by t-test (n = 5 rats).

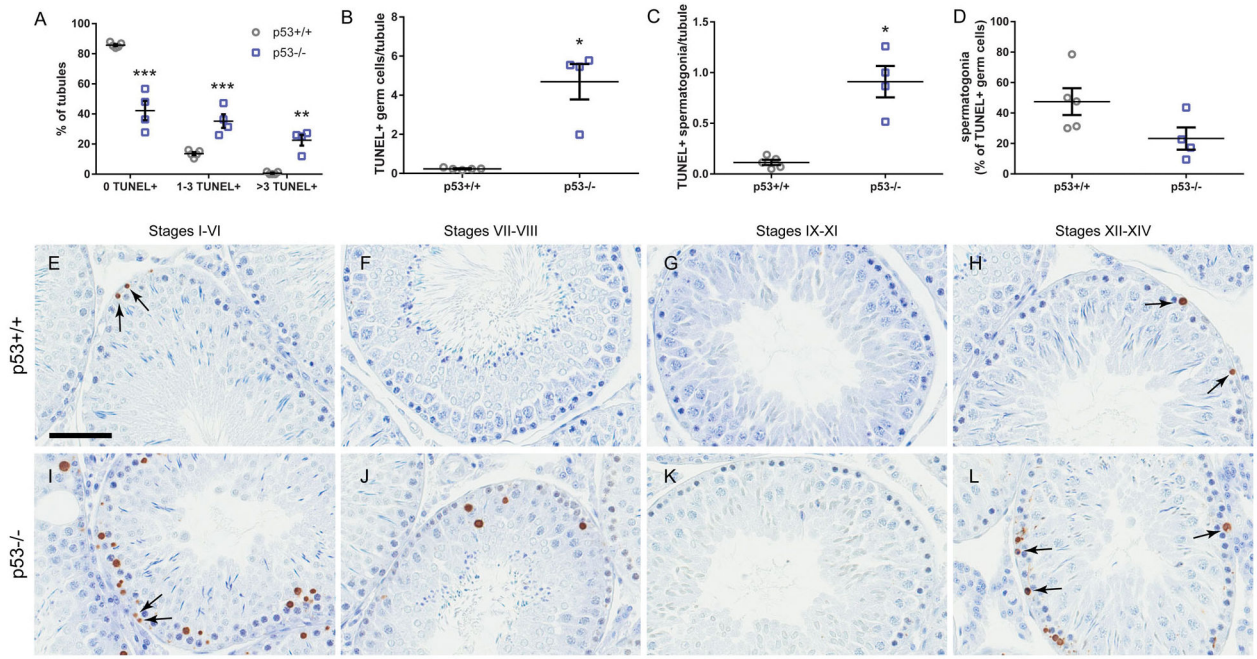

Figure 4.

p53−/− rats have elevated rates of testicular germ cell death compared to p53+/+. Compared to p53+/+, p53−/− rat testis exhibits significantly increased rates of TUNEL-positive germ cells (mean ± SEM) (A), particularly TUNEL+ spermatocytes. 33–77 tubules were scored per histological section of left testis from each animal (mean = 59.3 tubules). Atrophic tubules were excluded from the analysis. p53−/− testes had a greater number of TUNEL+ germ cells (B) and spermatogonia (C) per tubule than p53+/+ testes. The mean number of spermatogonia among TUNEL-positive cells trended higher in p53+/+ testes (not significant). ***, adjusted $p < 0.001$, ** adjusted $p < 0.01$ by multiple t-tests with Holm-Sidak multiple test correction. *adjusted $p < 0.05$ by Mann-Whitney U-test (n = 5 p53+/+ and 4 p53−/− rats). In p53+/+ rats (E–H), TUNEL+ spermatogonia (arrows) were frequently detected in stages I–VI (E) and XII–XIV (H). In p53−/− rat testes (I–L), TUNEL+ spermatogonia (arrows) were also detected, predominantly in stages I–VI (I) and XII–XIV (L). TUNEL+ spermatocytes were prevalent in all stages except IX–XI (K). Counterstained with methyl green. Scale bar = 60 μm.

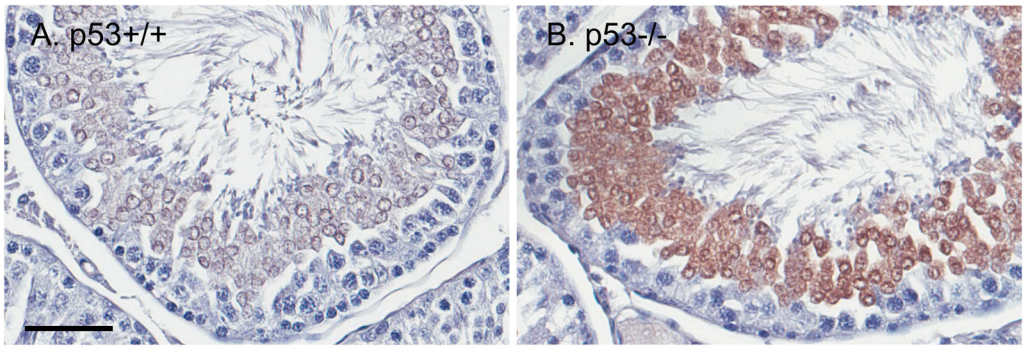

Figure 5.

Cleaved caspase-3 is localized predominantly to round spermatids in stages VII–VIII, both in p53+/+ (A) and p53−/− (B) rat testes. In p53+/+, cleaved caspase-3 is moderately intense and clearly expressed in the cytoplasm and perinuclear region. In p53−/−, cleaved caspase-3 intensity is often greater, and includes spermatids with apparent nuclear expression. Scale bar = 50 μm. Hematoxylin counterstain.

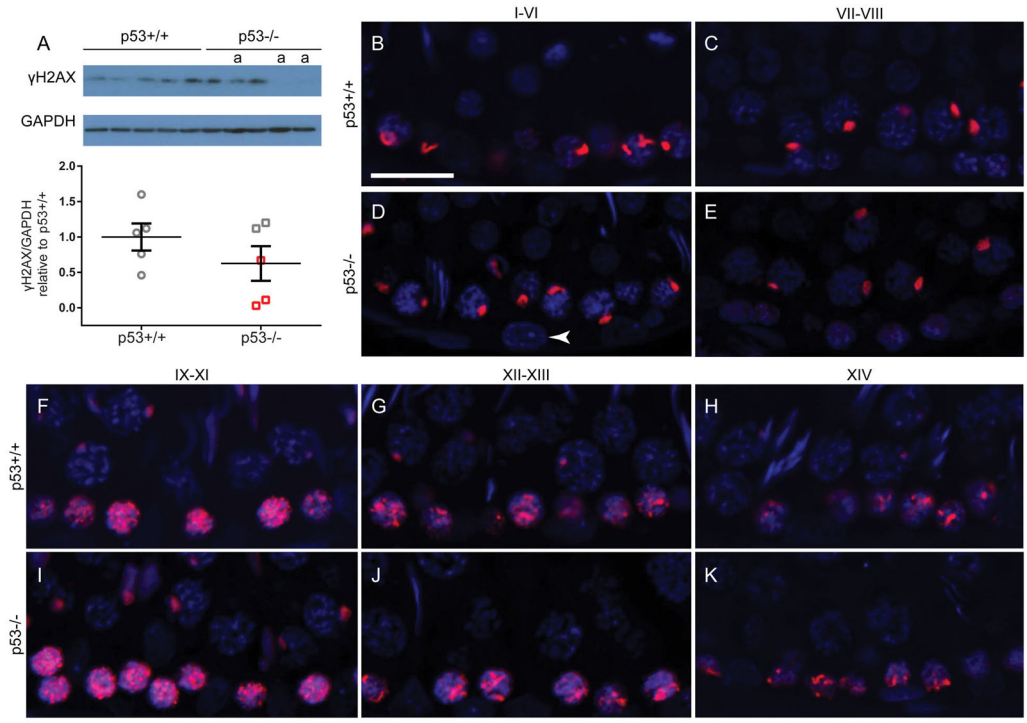

Figure 6.

γH2AX levels do not differ between p53+/+ and p53−/− rat testes. Western blot analysis indicated no significant difference in γH2AX protein quantity (mean ± SEM) between p53+/+ and p53−/− rats (t-test, n = 5 rats) (A). Lanes labeled with “a” are at least 50% atrophic. Red boxes correspond with atrophic samples labeled on Western blot. Immunofluorescent images of testes stained for γH2AX (red) and Hoechst counterstain (blue) indicate that the pattern of γH2AX localization is similar in the wild-type testis (B, C, F–H) and non-atrophic p53-knockout testis tubules (D, E, I–K). In stages I–VI and VII–VIII (B–E), γH2AX is present in the sex vesicles of pachytene spermatocytes. During stages IX–XIV (F–K), a large number of γH2AX foci are present in leptotene spermatocytes (IX–XI), becoming more focused in zygotene spermatocytes (XII–XIII), and condensing into the punctate sex vesicle stain in early pachytene spermatocytes (XIV). Spermatogonia do not show evidence of γH2AX presence in either genotype (e.g. white arrowhead in D). Scale bar = 20 μm.

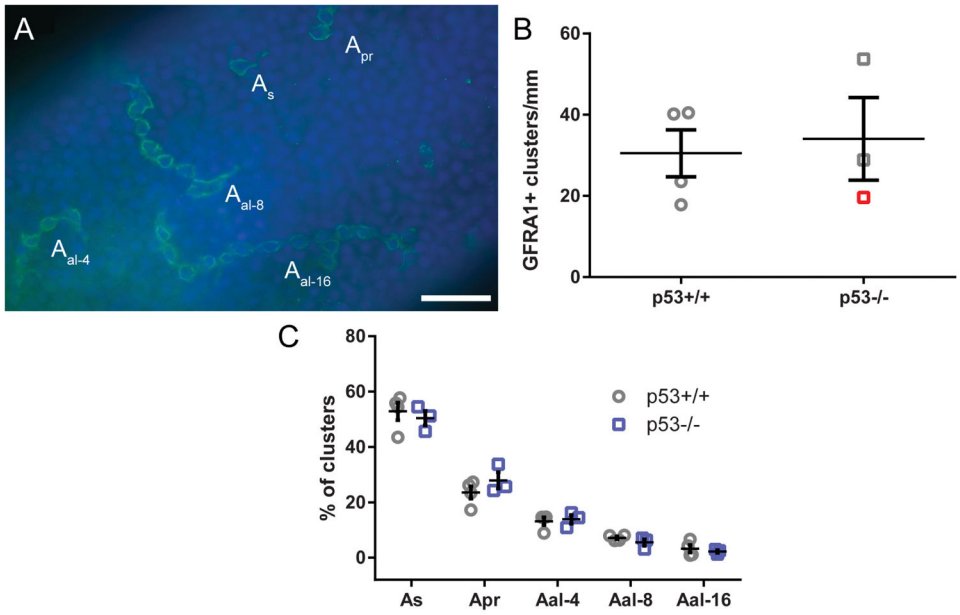

Figure 7.

GFRA1 staining and spermatogonial proliferation in p53−/− rats. Wild-type and knockout rat seminiferous tubules were isolated and GFRA1 was labeled using indirect immunofluorescence (green), with DAPI nuclear counterstain (blue) (A). Scale bar in A = 50 μm Tubules were examined for proportions of isolated (A_s), paired (A_{pr}), and longer-chain type A spermatogonia ($A_{al–4}$, $A_{al–8}$, and $A_{al–16}$). There was no significant difference in the number of clusters per mm seminiferous tubule (mean ± SEM, t-test) (B). Red symbol represents >50% atrophic testis. There was also no significant difference in the frequency of any category of cluster (mean ± SEM, multiple t-tests with Holm-Sidak multiple test correction, n = 3–4 rats) (C).

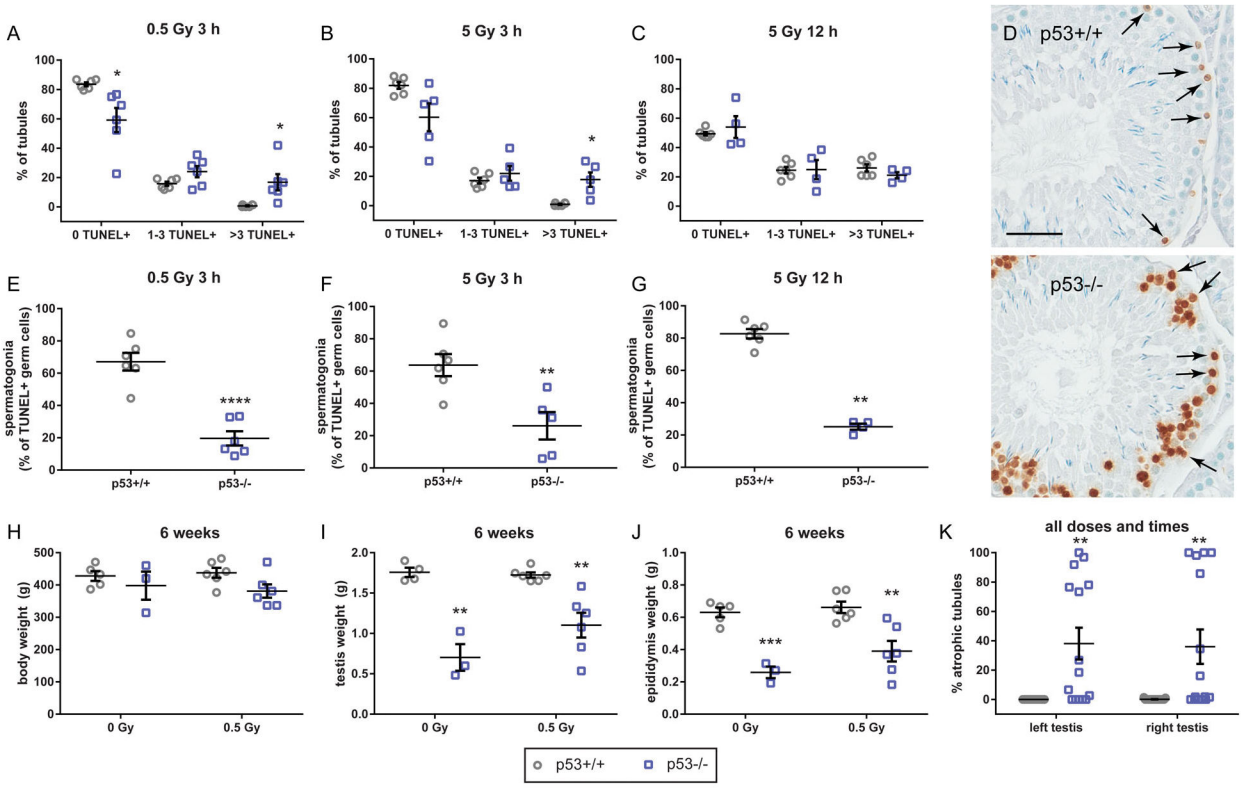

Figure 8.

Effects of X-radiation in p53−/− and p53+/+ rats. Following 0.5 Gy X-ray exposure (A) and 5 Gy X-ray exposure (B), TUNEL rates are significantly higher in p53−/− than p53+/+ rat testis sections (left testis). 12 h after treatment, 5 Gy X-ray treatment produced TUNEL rates that are statistically indistinguishable by genotype (C, right testis). At 12 h after treatment, TUNEL+ spermatogonia (arrows) are present in both p53+/+ and p53−/− tubules, especially in stages I–VI. However, p53−/− tubules also show significant numbers of TUNEL+ spermatocytes (D, scale bar = 50 μm). The proportion of all TUNEL+ cells comprised by spermatogonia was significantly greater in p53+/+ rats than p53−/− rats at all treatments and time points (E–G). Body weight was not significantly different between genotypes on postnatal day 97–102 (6 weeks after X-ray exposure) (H). Right testis (I) and right epididymis (J) weights in p53−/− rats were significantly lower than those in p53+/+ rats, 6 weeks after 0 Gy control or 0.5 Gy X-ray treatment. In all treatment groups and time points, seminiferous tubule apoptosis is observed in p53−/− rats significantly more frequently than p53+/+ rats, and is observed both in the left testis (3 h time point) and right testis (12 h or 6 week time points) (K). *adjusted $p < 0.05$, ** < 0.01, *** < 0.001, **** < 0.0001; A–C and H–J data analyzed by multiple t-tests with Holm-Sidak multiple test correction (n = 3–6 rats per group). E and F analyzed by unpaired t-test. G analyzed by Mann-Whitney U-test due to small sample size. H analyzed by two-way ANOVA followed by Sidak's multiple comparison test (n = 15–17 rats/group). All data reported as mean ± SEM.

Table 1

Stem Cell Proliferation.

Rat #	% atrophic tubules	# SSCs	# BrdU-labeled SSCs	Proliferative Index
1	76.7%	16	6	0.375
2	100.0%	19	7	0.368
3	1.3%	0	0	n/a
4	39.3%	0	0	n/a
5	0.6%	0	0	n/a

Serial sections were scored for percentage of atrophic tubules then examined for presence of spermatogonial stem cells (SSCs). Proliferative index was calculated, defined as the percentage of SSCs that were positively labeled for BrdU.